PHOTOMASK

BACUS—The international technical group of SPIE dedicated to the advancement of photomask technology.

Spatially-resolved dissolution monitoring using AFM

Luke Long and Andrew Neureuther, University of California Berkeley, Center for X-ray Optics, Lawrence Berkeley National Lab; **Patrick Naulleau**, Center for X-ray Optics, Lawrence Berkeley National Lab; **Jiajun Chen and Paul Ashby,** Molecular Foundry, Lawrence Berkeley National Lab

ABSTRACT

Continued lithographic scaling using high-NA EUV scanners requires materials and processes with sufficient resolution and stochastic performance to translate the aerial image into thin film photoresist material. Amongst these key processes is photoresist dissolution which converts latent exposure chemistry in the photoresist into a developed pattern. However, co-optimization of resist materials and the development process is difficult due to the challenge of directly measuring resist dissolution at the nanometer spatial and sub-second temporal scales on which it occurs. Most metrology of the dissolution process thus ignores either the temporal component by measuring just the final developed structure or the spatial component as is done in most dissolution rate monitoring experiments. To overcome these challenges, we have developed an in-situ dissolution rate monitoring technique using high-speed atomic force microscopy (AFM). As opposed to pioneering work using AFM to monitor the dissolution process, our technique incorporates the use of a specially designed flow cell which provides precise control of the time at which the developer is introduced to the photoresist material, as well as delivery of nearly full-strength developer in fractions of a second. Our system thus offers the ability to probe the spatially dependent nature of the dissolution process at conditions close to those in the fab, providing insight into exposure-dependent dissolution rate gradient, material swelling, and other potentially lithographically relevant phenomena such as polymer entanglement. In doing so, we provide another technique to aid in the design and study of photoresist materials for future lithographic nodes.

1. INTRODUCTION

With EUV being actively used in high-volume manufacturing (HVM), the industry looks to high-NA scanners to continue the progression of transistor shrinkage. However, the ability to manufacture ever-smaller transistors relies critically upon having photoresist materials and manufacturing processes capable of resolving the aerial images delivered by the scanner to the wafer. To that end, the industry as a whole has made valiant efforts in improving all aspects of the process, from a novel, resist materials1 to underlayer materials[2,3] and even material processing and deposition.[4] Despite these efforts, the workhorse material system used in HVM is still chemically amplified resist with 2.38*wt%* TMAH as a developer.

Previous studies of dissolution using TMAH as a developer hint at the presence of swelling prior to the removal of photoresist material. For example, the quartz crystal microbalance (QCM) technique,[5] has been used to measure the dissolution response of photoresists exposed to clear-field or unpatterned radiation,

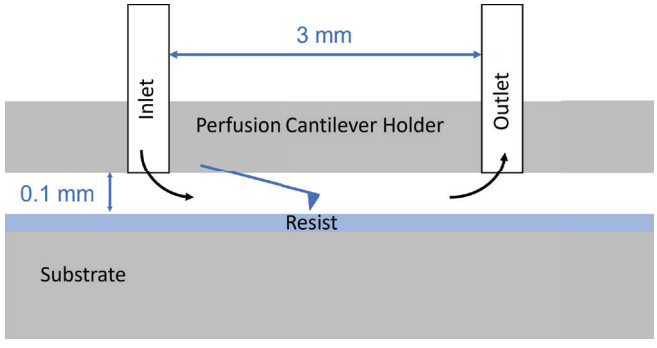

Figure 1. Schematic of the flow cell created by the perfusion cantilever holder and the substrate.

BACUS NEWS

DECEMBER 2022
VOLUME 38, ISSUE 12

TAKE A LOOK INSIDE:

SPIE.

12292-7

EDITORIAL

Photomasks, ski swaps, and the surprising similarities

Jed Rankin, IBM

I am blessed that living in Vermont I am surrounded by mountains and ski areas that fuel my love of skiing. Every fall, my family and I volunteer at a local ski swap hosted by a non-profit family ski area where neighbors can exchange a used pair of skis or donate a snowsuit that the kids have long since outgrown. These ski swaps give an opportunity for the ski community, consisting of skiers, ski suppliers, and the ski mountains to keep costs down, help people empty garages, and minimize waste. For the last two years, COVID-19 required us to change to a virtual online format. The ski community supported the virtual swap, but since the clothes cannot be tried on or ski quality assessed in person, sales volumes dropped significantly. This year marked the return of the in-person ski swap, where once again buyers could try on the boots, feel the ski edges, and catch up with old friends to reminisce about past snowstorms and dream of the ones to come.

Another event, I look forward to in the fall is the annual BACUS and EUVL photomask conference, which also returned to an in-person event this year after a two-year COVID-19 driven hiatus. Presentations overflowed with amazing EUV and mask technology that is no longer a dream, but firmly in production reality. The excitement for the technology was hard to contain. Everywhere you looked, it was great to see the community back together with colleagues and friends chatting during breaks, having meetings between sessions, or even doing a little karaoke late into the night!

When asked to report on the conference, my summary was simply: EUV Lithography Works. This is of course a simplification and an injustice to the decades of hard work by so many dedicated scientists and engineers as they have repeatedly overcome dozens of "insurmountable problems". The perennial sentiment had been that EUV was poised for production next year. This year the change in the message was stark - defect-free blanks are a reality, actinic inspection tools for blanks and masks are readily available, multibeam mask writers are in production, EUV pellicles are being commercialized, and 13.5nm AIMS tools are available! When asked to expand on my brief statement, I added that it takes a LOT of money, and has only been done by fabs with captive mask shops. High Volume Manufacturing EUV mask production does not come cheaply.

High-NA EUV has been in the planning for several years. It was exciting to see the amount of work that has already been done in preparation for the next-generation of High-NA scanners. Many teams and organizations are already working on the blanks, films, masks, and tools that will enable and leverage High-NA EUV. With Low-NA EUV already in production, the sentiment was clear that despite the challenges, High-NA challenges are all surmountable with investment.

Last weekend, while volunteering at the ski swap, another similar problem shared by skiing and EUV lithography struck me: rising costs and large initial investment requirements. It is a common complaint that skiing is becoming an "elitist sport" due to high the cost of lift tickets, equipment, clothes, and travel. There is generally worry that these costs and waning interest may undermine the viability of future technical development.

Commercial maskshops produce many EUV masks to develop, enable, and characterize the scanners. To this point, only IDMs possessing captive maskshops have successfully enabled manufacturable EUV lithography, and EUV mask production. This has left no commercial foundry market for HVM EUV masks. The support of the fabs in pursuit of next-generation technology has enabled the captive maskshops to justify the risk and make the investments necessary to support HVM EUV mask production – is EUV also an elitist sport?

One of the biggest and most discussed topics in the panel sessions was mitigating the limits of ½ field masks mandated by the anamorphic optics. Full-field anamorphic masks would require a new form factor; one option is potentially using 300mm round substrates. Optimistically, some members of the audience guessed that redeveloping substrates, tools, and processes would take 5-7 years, not to mention the hundreds of millions of dollars required.

Looking out of my window, I see the first snow of the year is starting to pile up. While it seems likely that high volume IDMs will likely be able to justify the cost of High-NA, I wonder if the cost of 300mm round masks will be containable? What about for the commercial mask makers? How will they justify and offset the costs without commercial HVM customers? What materials will we be using and developing in 5 years? What new challenges and opportunities will High-NA exposures reveal?

These problems will be solved. Researchers, mask shops, foundries, fabs, and tool-makers will figure out the science and the economics. I am excited to meet with my peers and friends at future BACUS and EUVL conferences. Together we will bemoan the challenges of mask-making, celebrate the novel ideas, and speculate on the challenges to come. For now, I think I'll get my new-to-me skis and go spend some time alone in the woods.

BACUS

N • E • W • S

BACUS News is published monthly by SPIE for *BACUS*, the international technical group of SPIE dedicated to the advancement of photomask technology.

Managing Editor/Graphics Linda DeLano
SPIE Sales Representative, Exhibitions, and Sponsorships Melissa Valum
BACUS Technical Group Manager Tim Lamkins

SPIE.

P.O. Box 10, Bellingham, WA 98227-0010 USA
Tel: +1 360 676 3290
Fax: +1 360 647 1445
SPIE.org
help@spie.org

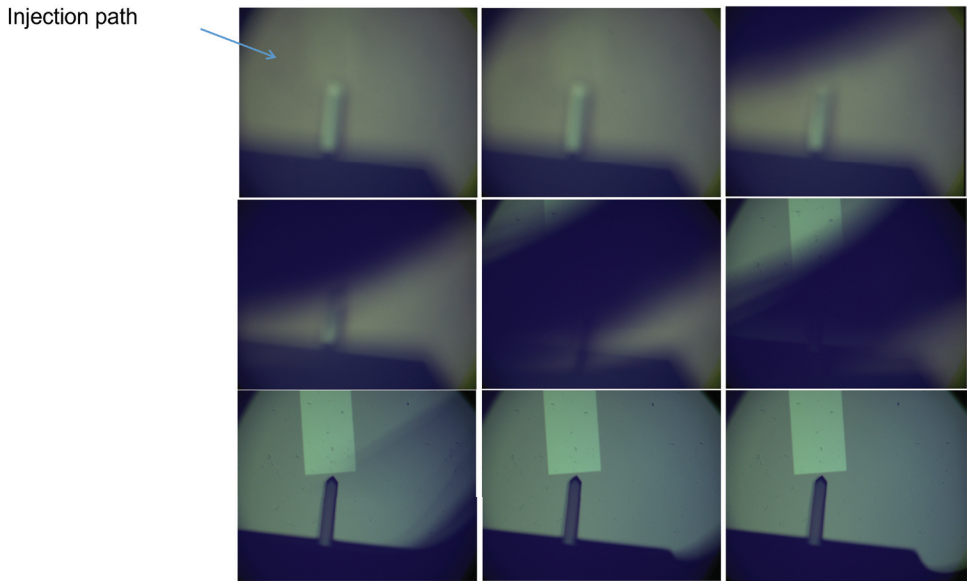

Figure 2. Optical images of the cantilever tip during an early attempt to flow TMAH while imaging using the default perfusion holder. The increase in optical contrast of the exposed rectangle after the occlusion passes over the cantilever is evidence that the sample has developed. Imaging is not possible while sight of the cantilever is occluded.

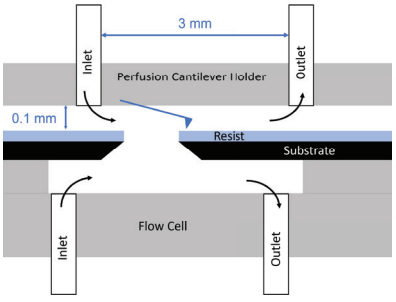

Figure 3. (a) Schematic of the flow cell. Two channels allow two fluids to be located near the sample such that full strength developer can be delivered to the resist without complete displacement of the initial fluid.

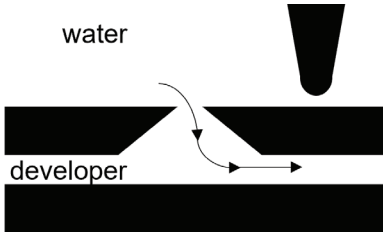

(b) Schematic of the initial flow conditions. Fluid inert to the resist flows from the top channel to the bottom, sequestering developer below the substrate.

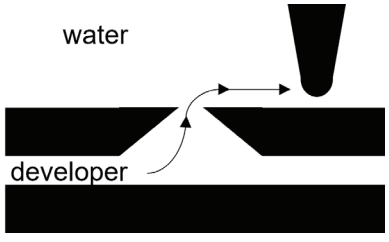

(c) Schematic of the final flow conditions. Flows are changed such that developer is forced from the bottom channel up to the top. The close proximity of the sample to pore separating the channels results in rapid delivery of full strength developer.

showing a brief swelling of the resist before its rapid removal.[6] Similarly, Itani et al. performed AFM experiments measuring the dissolution response of patterned resist materials and also observed swelling prior to the removal of the exposed material.[7] This swelling may be a significant contributor to LER, and has been cited as a motivating factor in the search for novel developers, including a tone-switch by using solvent developer.[8,9] However, previous AFM work has required significant dilution of the developer solution to enable observation of the dissolution process. It is unclear whether the dynamics of dilute dissolution are representative of those of full-strength developers.

In this work, we present on our progress in developing a technique for spatially resolved measurement of photoresist dissolution using a full-strength developer. We discuss the key enabling factor, a specially designed flow cell that allows for precise control over the injection of the developer solution and highlights some of the practical difficulties encountered along the way. We present several of our most recent results, showing our ability to measure the dissolution of line-space patterns at the single-digit nanometer and sub-second temporal scale, as well as our ability to track key lithographic metrics such as line edge roughness as a function of dissolution time. We present some of our fastest imaging to date, achieved by scanning the AFM probe across the sample in a non-raster pattern.

2. MATERIALS AND METHODS

2.1 Materials

For the purposes of technique development, a commercially available CAR resist was used throughout the results presented in this paper. The resist is known to be a relatively high-resolution material, with a correlation length of about 15*nm*. The resist was patterned using 100*keV* electron beam lithography, with a dose size of around 220uC/cm^2. The dose to clear the same material to EUV radiation is around 12mJ/cm^2.

The developer used in this study was ma-D 525 from micro resist tech-

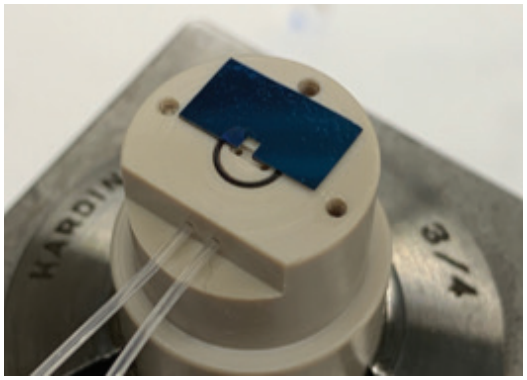

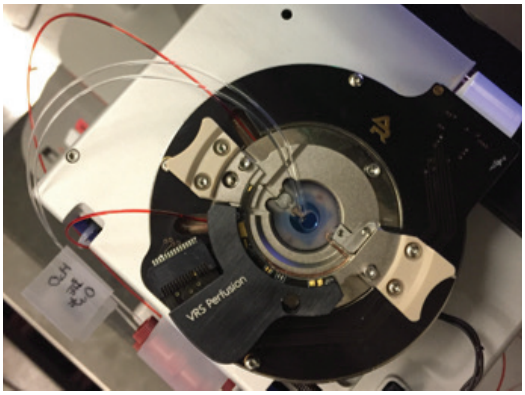

Figure 4. (a) Early version of the flow cell, still on the lathe. Adhered to the flow cell is a cross-sectioned SiNx membrane; a full frame with a punctured window forms the pore between channels.

(b) Closed flow cell. The Cypher VRS perfusion holder forms the top of the flow cell. Clear lines correspond to the inlet and outlet of the top channel, while the red lines correspond to the inlet and outlet of the bottom channel of the flow cell, dyed red here for diagnostic purposes.

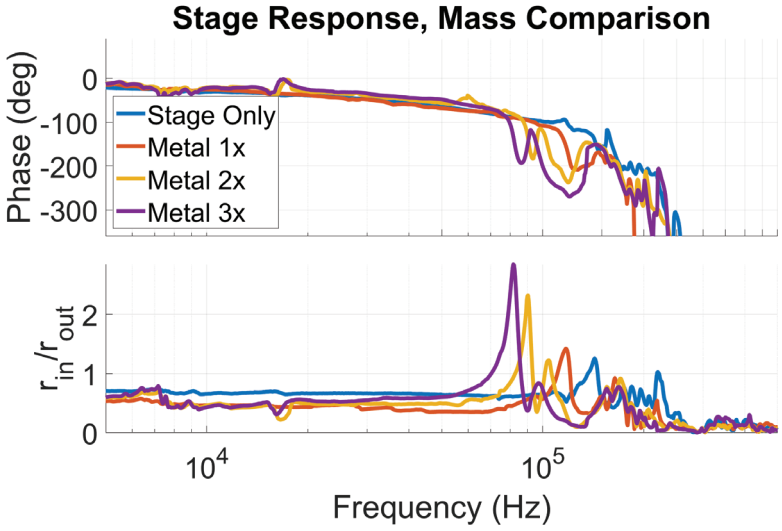

Figure 5. Frequency response of the z-piezo as a function of mass. As more mass is adhered to the stage, inertial effects lower the resonant frequency of the pizeo. As this resonance causes imaging to be unstable, amplitude signals at and above the resonant frequency must be filtered, which results in filtering of the resulting image.

nology, a 2.38% solution of TMAH without surfactant.

2.2 Atomic Force Microscope

The AFM used to perform these experiments is the Cypher VRS from Asylum Research. The VRS module enables high-speed imaging through its stack of z-peizos: one for the course, slow height modulation over relatively large length scales, and a second for fine, fast modulation. The VRS perfusion cantilever holder assembly was used for this study, which offers the minimum distance between the liquid inlet/outlet of the commercially available holders.

2.3 Flow cell

A major challenge with in-situ measurement of photoresist dissolution is that the experiment must be set up in a liquid environment, as the presence of fluid affects the mechanical characteristics of the cantilever oscillation as well as the optical properties of the imaging system responsible for measuring the cantilever motion. This starting liquid must not dissolve the resist and must be replaced by the developer in order for dissolution to occur. A diagram showing the default liquid channel created by the sample and cantilever holder is shown in Figure 1. The issue with this setup is twofold. First, due to the relatively large distance between the liquid inlet/outlet in the cantilever holder, the concentration of developer that reaches the sample changes as a function of time; the displacement of the starting fluid (normally water) by the developer is accompanied by a front in which the two fluids have mixed, creating a concentration gradient. This makes it difficult to assign the dissolution phenomena to any particular concentration of developer.

An even greater challenge is posed by the optical disturbance created by the mixing of the two fluids. Figure 2 shows the result of an early attempt at performing a full-strength dissolution experiment using AFM. Here, the dark shadow that passes over the optical image of the tip and sample comes from the incoming developer front. This shadow occludes the optical feedback that measures the cantilever motion, which in turn provides the information used to adjust the height of the sample relative to the tip, ultimately producing the topographic map of the sample. Once the water has been effectively displaced by the developer, the occlusion passes. However, during this brief time, the resistance has more

Figure 6. Current flow cell. Excess mass has been removed to push the resonant frequency of the piezo-flow cell system as high as possible.

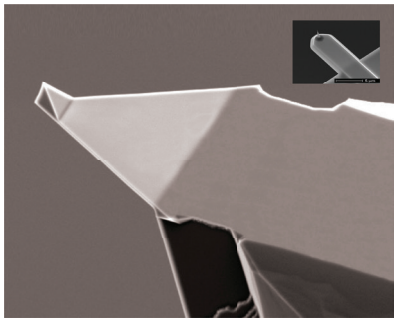

Figure 7. SEM images of two different probes used for dissolution experiments. The large image is the Arrow UHF probe. The small probe in the inset, approximately to scale, is the USC f1.2 k0.15 probe, which is preferable to the Arrow UHF for studying soft polymers due to its lower stiffness, but presents challenges for the feedback laser due to its reduced size.

Table 1. Comparison of AFM probe parameters. f_0 is the frequency of the first harmonic in air, *k* is the probe stiffness, *L* is probe length and < W > is the average probe width. Note the substantial drop in stiffness for the USC f1.2 k0.15 probe relative to the UHF Arrow, and the corresponding drop in probe dimensions.

	UHF Arrow	USC f1.2 k0.15
f_0	1.5MHz	1.2MHz
k	8N/m	0.15 N/m
L	35μm	7μm
< W >	42μm	2μm

or less completely developed. Measurement of the key dissolution dynamics is thus missed during the fluid exchange process.

To overcome these issues, a special flow cell was designed. As shown schematically in Figure 3a, the flow cell is designed to have two separate channels separated by a small pore. The top channel is initially filled with the starting fluid (i.e. water), while the bottom channel is filled with a developer (i.e. TMAH). The pore is created using a punctured silicon nitride membrane. The sample to be studied, in this case, patterned photoresist, is placed right next to the window. The experiment is set up such that, initially, water is forced from the top channel through the pore to the bottom channel, sequestering the developer in the bottom channel (Figure 3b). Then, using microfluidic pumps, the pressure is changed at the desired time to force the developer from the bottom channel through the pore to the top channel (Figure 3c). Due to the proximity of the patterned resist and the pore, the developer that is introduced to the sample is nearly instantly at full concentration. Furthermore, as the developer is coming from below the tip, the occlusion effect mentioned above is minimized (though not completely eliminated, as discussed in Section 2.6).

An early version of the flow cell is shown in Figure 4a. The cell is made of polyether ether keytone (PEEK), in which the developer-containing channel is milled. Figure 4b shows the fluid cell closed, with the water inlet/outlet at the top of the cantilever holder. During an experiment, the flow cell is epoxied to the sapphire surface of the Cypher VRS stage for scanning.

2.4 Z-piezo Response

The imaging modality used for the in-situ AFM study is known as amplitude modulation tapping mode. In this mode, the amplitude of the cantilever oscillation is held constant by moving the sample closer to or further from the tip during the scan according to the topography of the sample. In the Cypher AFM, all of *x*, *y*, and *z* motions are handled by piezos that displace the sample relative to the tip. In the Cypher VRS, there are in fact two *z* piezos, a "slow" piezo, responsible for the bulk motion of the sample, and a "fast" piezo that makes the small adjustments at high speed that enable video-rate scanning. However, the frequency at which the z-piezo can respond to changes in cantilever oscillation amplitude is limited by inertial factors that create a sort of resonance in the piezo response. The resonant effect leads to a delay in the z-position of the stage relative to the amplitude signal, and furthermore, to an over-correction of the z-stage position, which together conspires to destabilize the imaging. Thus, amplitude signals that occur near or above the resonance must be filtered in order to avoid unwanted stage motion, at the expense of tracking the high-frequency features of the image. As the frequency at which the amplitude of the tip changes is directly related to the speed at which the sample is being scanned, the max stable imaging rate is effectively set by a combination of the desired frame rate, and the fidelity with which the tip tracks over the sharp changes in sample topography (such as that at the edge of line/space pattern).

To test the frequency response of the z-piezo, a series of different masses in the form of stainless-steel disks have adhered to the VRS stage. A tip was brought into contact with the disks. The z-piezo was then driven by an external waveform generator, and the frequency swept across the expected resonance. The deflection signals coming from the tip, being in contact with the sample, is thus a measure of the resulting motion of the piezo relative to the drive signal. Figure 5 shows the result of this experiment. In the absence of any additional mass, the stage shows a small resonance just above 100*kHz*. However, as additional mass is added to the piezo, the frequency of the resonant behavior drops to around 65*kHz*. This result, combined with observed instability during preliminary dissolution experiments, motivated trimming away extra PEEK material from the flow cell. The resulting flow cell is shown in Figure 6. Despite the improved frequency response of the trimmed-down liquid cell, we have empirically found it necessary to filter all amplitude signals above about 45kHz in order to maintain stable imaging.

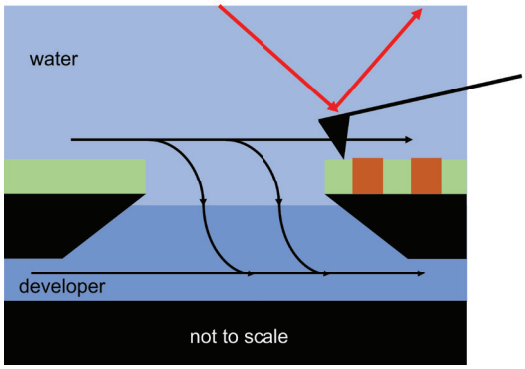

Figure 8. (a) Initial flow conditions. The subtly more dense developer solution is sequestered below the tip. Laser feedback and scan parameters are established.

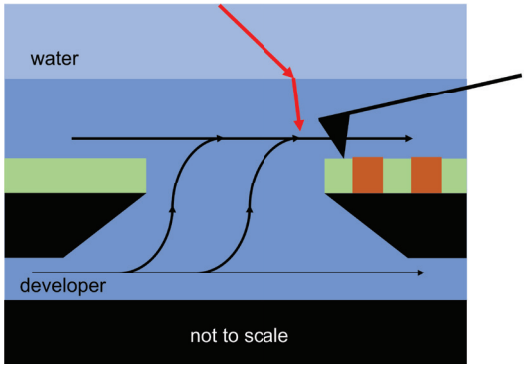

(b) Flow conditions are switched such that the developer is introduced to the top channel. The subtle change in the index of refraction causes the laser to miss the cantilever. Tracking is lost.

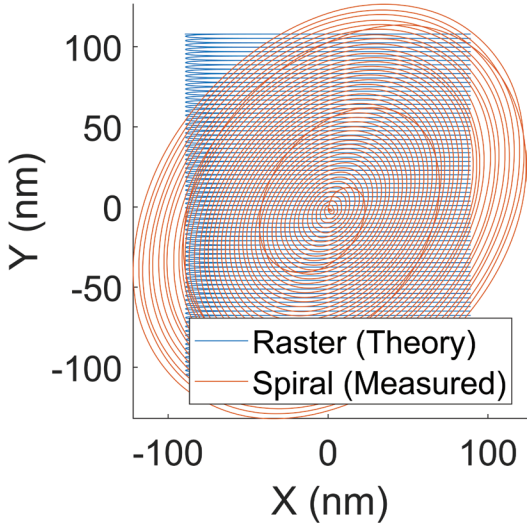

Figure 9. (a) Comparison of two scan patterns covering approximately equal area. In blue is the standard raster scan, while in red is the spiral scan pattern.

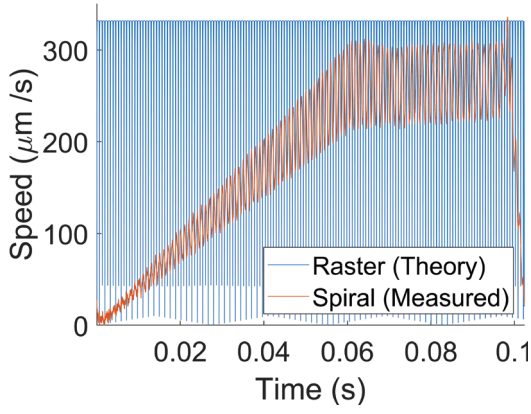

(b) Comparison of the speed as a function of time required to scan the two patterns. Due to stopping at the edge of each scan line, the raster pattern needs a higher average and max speed to achieve the same frame rate as a spiral scan, which is constantly in motion.

2.5 AFM cantilever

For high-speed AFM measurements, it is desirable to have a cantilever with a high resonant frequency, such that the feedback has several oscillations worth of amplitude data per pixel. In our experiments, our earliest results were achieved using the Arrow-UHF probe shown as the large image in Figure 7. Tip parameters are shown in Table 1. This primary issue with this tip is that it is relatively stiff; when imaging over the soft polymer surface created by the photoresist, the tip tended to cut into the sidewalls of the resist, particularly when imaging at high speeds. A more appropriate tip for soft resist materials is the USC F1.2 k0.15 probe shown in the inset of Figure 7, approximately to scale with the Arrow-UHF. This tip has a similar in-air resonant frequency, but with a much lower stiffness. However, to achieve both high frequency and low stiffness, the tip must be made much smaller than its Arrow-UHF counterpart. As discussed in Section 2.6, this had repercussions for the stability of imaging.

2.6 Fluid Mixing and Index Matching

As mentioned in Section 2.5, early results were achieved with the Arrow-UHF cantilevers, but the smaller USC cantilever is preferable. However, our early attempts at using these tips were foiled by loss of tracking during the injection of the developer. In fact, as highlighted in Section 3.1, even our most successful early attempts with the Arrow-UHF tips suffered from some instability as the developer was injected. After much troubleshooting and a number of failed experiments, the root cause of the problem was uncovered. It turns out that, just as our early attempts using the standard VRS pefusion cell setup failed due to mixing-induced occlusion of the AFM tip, our new flow cell design suffered from some minor optical disturbances caused by differences in the index of refraction betweem developer and water. As shown schematically in Figure 8, the developer solution, a mixture of TMAH salt and water, is subtly more dense than water. As a result when the developer is introduced to the top flow channel, the index mismatch forms a sort of lens that causes a small deflection of the feedback laser, particularly when the developer is first injected. While the effect is much less dramatic than the situation without our flow cell, the small deflection is still sufficient to cause the laser to miss the very small cantilever onto which the laser is focused.

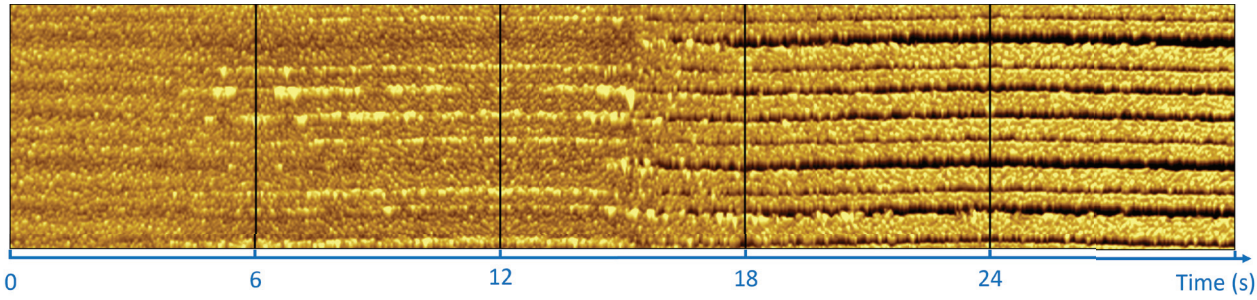

Figure 10. Early result captured at 6s/frame using a flow condition that leads a low developer concentration. Low concentration leads to swelling of photoresist, consistent with prior findings.

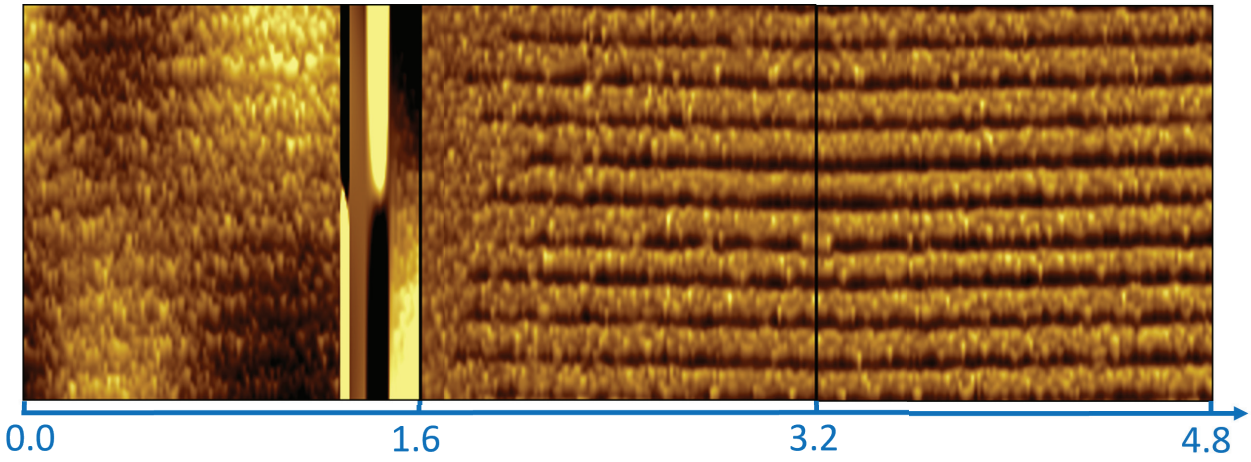

Figure 11. Early result captured at 1.6s/frame using a flow condition that leads to nearly full-strength developer. No swelling was observed, but tip tracking was lost for a few scan lines as the developer was injected.

To solve the problem, we decided to start with a fluid with an index of refraction near that of the developer. We selected a 2.38*wt%* solution of NaCl due to its availability and its neutral pH of 7. Several control experiments were conducted, which suggested that a pre-rinse with this solution prior to development had no discernible effect on the dose to clear or dose to the size of the commercial CAR used for technique development. The change from water to a weak NaCl solution as the beginning fluid proved to be the final change needed to really push the imaging speed limits of the technique and enabled the high-speed results presented in Section 3.2.

2.7 Spiral Scanning

As a final improvement, we changed the tip scan pattern from the default raster scan to a spiral scan as described by Zeigler et al.[10] As outlined in Section 2.4, due to the combination of additional mass from the flow cell as well as the intrinsic resonance of the z-piezo, high-frequency amplitude signals must be filtered in order to maintain stable imaging. Unfortunately, this filtering limits the resolution of the imaging process at high x-y scan speeds, as faster x-y speeds directly translate to higher frequency amplitude signals. Thus, for a given filter on the amplitude signal coming from the cantilever, there is a maximum scan speed that can be used, above which the height map (built from the z-peizo motion) loses its high spatial frequency information.

In a traditional raster scan, the velocity of the probe relative to the sample surface becomes very slow at the x extremes of the image, while the velocity is maximized throughout the middle of the scan pattern. As a result, to achieve a given frame rate, the scan speed between turnarounds must be greater in order to make up for lost time. In contrast, a spiral scan such as that described by Zieler et al.[10] enables scanning to be performed such that the probe is constantly in motion, maximizing the rate of useful data collection. As a result, a spiral pattern can be used to scan an equivalent area as a raster pattern using lower average and max velocities. A plot showing a theoretical raster pattern and an experimentally measured spiral pattern at a 10Hz frame rate is shown in Figure 9. As illustrated in the figure, the spiral scan enables lower scan speeds, which translates to improved image quality. This enables an increase in frame rate such that the sample dynamics can be probed at a greater temporal resolution for a given scan area and data density.

3. IMAGING RESULTS

3.1 Early Results

In our earliest results, collected with Arrow-UHF cantilevers and with pure water as the starting solution, we were able to reproduce the results of previous in-situ dissolution experiments using AFM. These results are presented in Figure 10. In particular, by using flow conditions that correspond to a weak developer solution, we see a significant swelling of the resist material prior to removal. However, by adjusting the flow conditions used to inject the developer, we were able to achieve a more full-strength develop. These results are shown in Figure 11. In this data, we did not observe swelling of the photoresist material. However, as hinted at in Section 2.6, we suffered from a few scan lines where the probe was not tracking the surface. The dynamics clouded by these few scan lines,

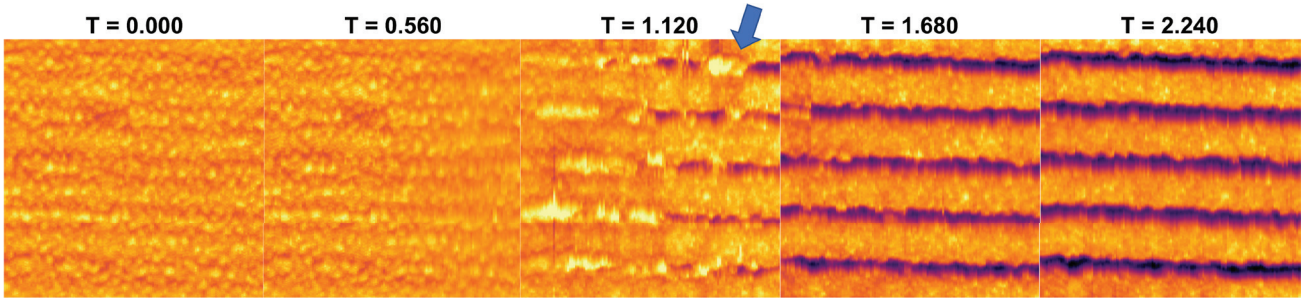

Figure 12. First high-speed imaging result using index matching and soft cantilever probe. Frame rate was 1.9Hz. Stable tracking throughout the development revealed that swelling does indeed occur at full-strength developer. Furthermore, swollen regions along the line edge appear to correlate with protrusions from the line edge, indicating the formation of LER.

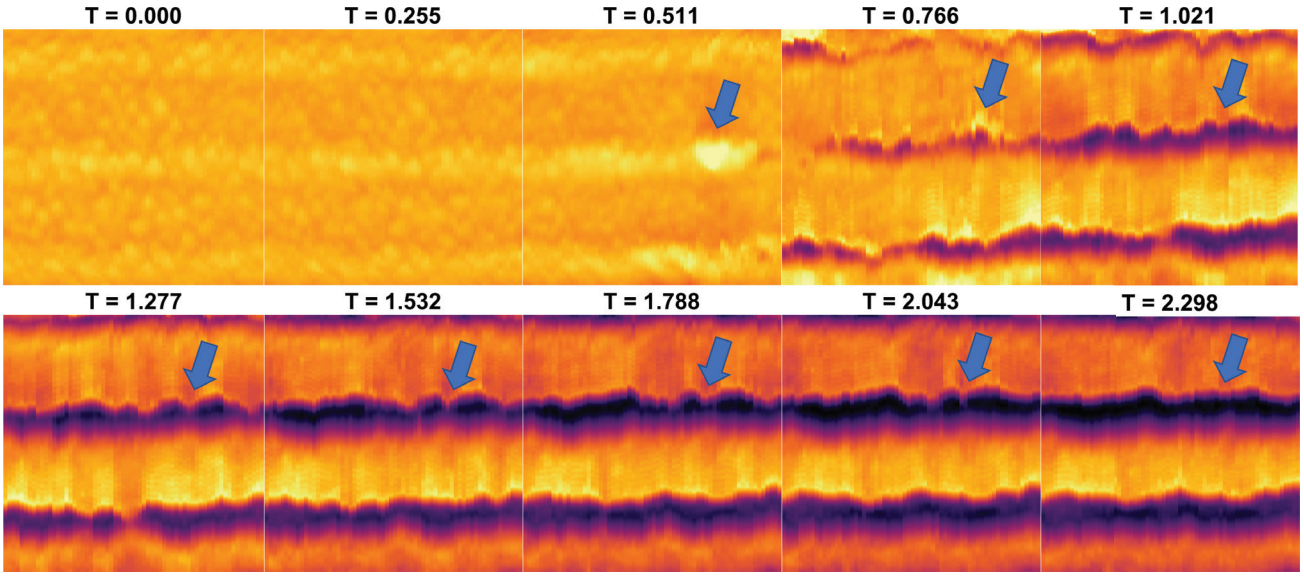

Figure 13. Dissolution data set collected at 3.9Hz. Scan area was reduced due to the imaging speed constraints set by the z-piezo. Finer temporal resolution reveals the gradual opening of the trench during development. As with the 1.9Hz data set, swelling preceeds removal of resist, with most swollen regions corresponding to bumps on the line edge. As development progresses, small bumps are smoothed out, suggesting that the developer serves to filter LER after the inital removal of material.

coupled with our confidence that we were not near the imaging speed limits of the instrument, motivated the improvements to the experimental technique that culminated in the data presented in the next section.

3.2 Latest Results

3.2.1 Raster Scan

By index matching and using a more appropriate tip, as outlined in Sections 2.5 and 2.6, we were able to stably image throughout the dissolution process. To test out the improved system, we studied 100*nm* pitch lines exposed via electron beam lithography at a 1:1 duty cycle. Our first result is shown in Figure 12, which was taken at a 1.9Hz frame rate. In this data set, each image is approximately 500*nm* x 500*nm*, with 128 total lines scanned sequentially from left to right in an image, yielding approximately 4nm pixels in the horizontal direction. Each line was scanned from the bottom to the top of the image, with the pixel size along this direction about 1nm. The developer was injected in approximately the middle of the second frame (T = 0.560). With the improved tracking and imaging speed, we were able to observe swelling during dissolution that our previous full-strength developer data did not reveal. Furthermore, we observed that, even in areas of the line that were nominally exposed to the same

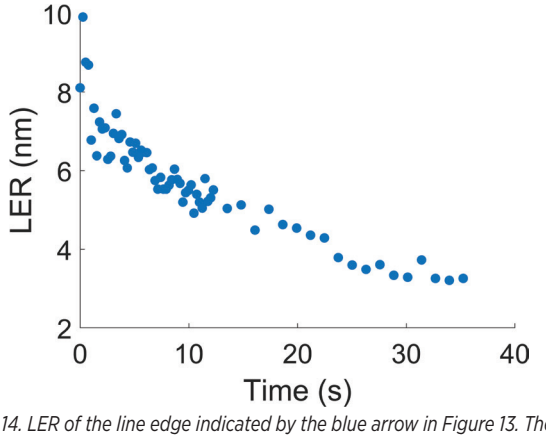

Figure 14. LER of the line edge indicated by the blue arrow in Figure 13. The line is roughest just after its formation and smooths as the developer works away at the partially exposed material at the edge. LER plateaus at around 30s, the process of record development time for this resist.

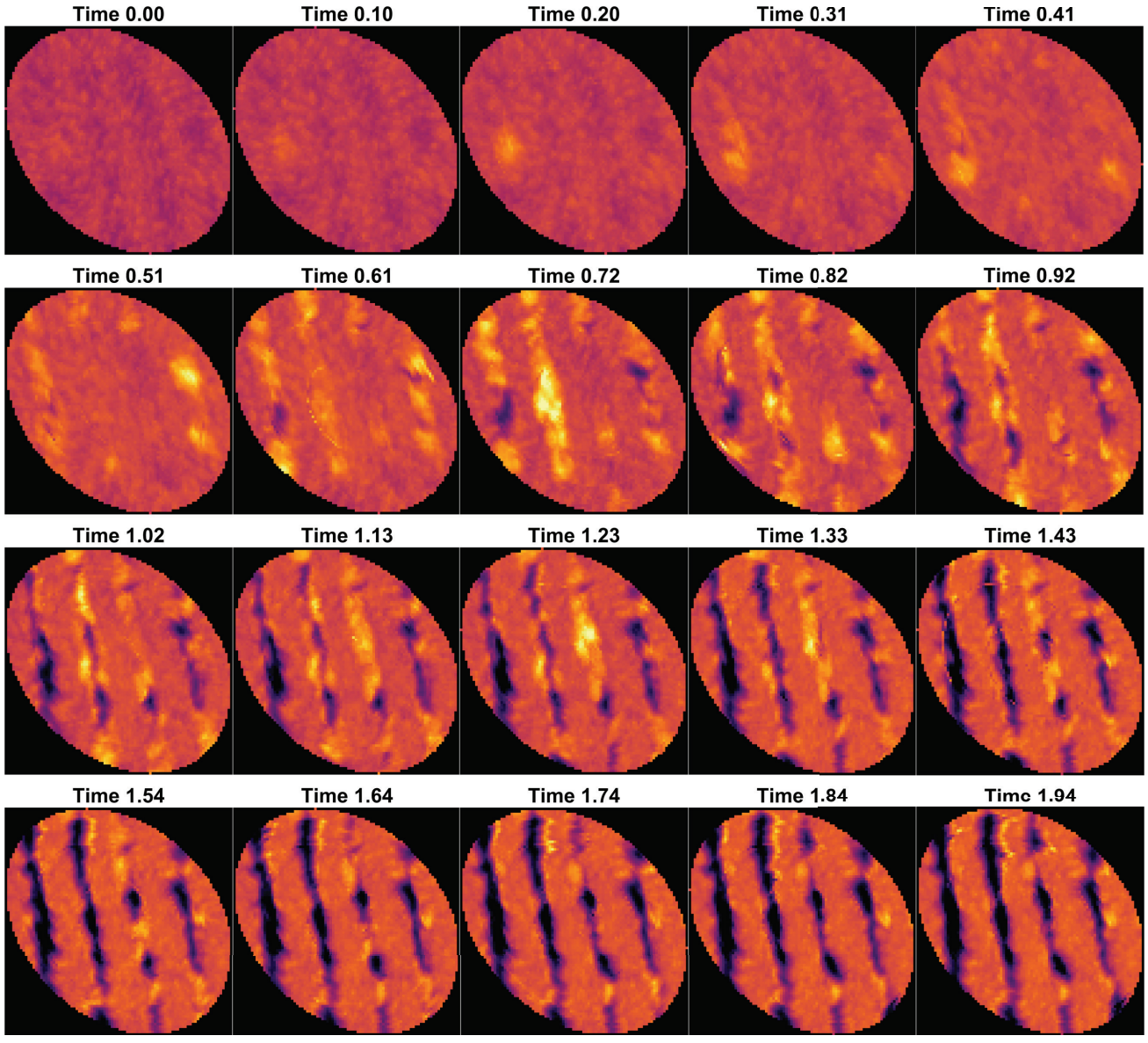

Figure 15. Data captured using a spiral scan pattern at 9.7Hz. With this level of temporal detail, it can be seen that the middle of the exposed feature swells and is removed most rapidly, leaving behind lesser-exposed swollen resist on the sides of the trench that is also removed as the development process proceeds.

dose, the swelling and dissolution appeared to occur at different times. For example, take the uppermost trench as it develops in Figure 12 in the frame T=1.12. Here, we see a blob of swelling, indicated by the blue arrow, that was measured later chronologically than the developed part of the line just to its left. This suggests that we are measuring inhomogeneity in the dissolution process, though at this stage we are unable to identify whether this comes from the electron beam exposure, material inhomogeneity, the developer, or a combination of all three. Interestingly, the swollen bump appears to leave behind a nodule on the line edge once the bulk of the material is removed, which is perhaps expected of an under-deprotected region of resist.

Intent on improving upon these results, we moved to imaging at a faster frame rate. However, due to the z-peizo limits highlighted in Section 2.4, this necessitated reducing the overall area being imaged. The resulting data is illustrated in Figure 13. In this data set, the frame rate was 3.9Hz, with each image having area 250*nm* x 250*nm*, 64 lines per frame, and equivalent pixel size and scan direction as the previous data set. Just as in the last data set, we again see the presence of swelling before rapid removal of the material. With the improved frame rate, it becomes increasingly apparent how the middle of the exposed region is removed first, followed by a gradual removal of the lesser-exposed resist surrounding the trench. In particular, one can track the material in the vicinity of the swollen bump indicated by the blue arrow. Just as in the previous data set, the removal of this swollen region leaves behind a nodule on the line edge. However, tracking that nodule throughout the development process reveals that the developer slowly removes the bump, leaving behind a smoother line edge. This is likely due to the fact that, once the bulk of the material is removed, the developer is able to interact with the resist not only from the top down, as is initially the case, but also from inside the developed parts of the trench, effectively increasing the dissolution rate of protrusions. To put some numbers to this effect, the line edge corresponding to this protrusion was fit using

SuMMIT,[11] and LER data extracted as a function of dissolution time. The results is shown in Figure 14. Matching the obvious visual effect, the LER of the line edge decreases rather rapidly near the beginning of the develop before saturating at a minimum value near 30*s*. It is worth noting that 30*s* is the develop process of record for this photoresist material.

Naturally, we wanted to make yet another improvement in our scan speed in an attempt to fully resolve the swelling and remove the resist material. However, even at the current frame rate, there were some artifacts introduced by the speed of the scan when transitioning from the top of the line to the trench, a phenomenon known in the AFM community as "parachuting". Furthermore, increasing the frame rate would require another reduction in the image area, representing a challenge at the 100*nm* pitch being measured here. To take the next step in frame rate, we moved to the spiral scan discussed in Section 2.7.

3.2.2 Spiral Scan

In conjunction with changing the scan pattern, we reduced the pitch of the pattern features from 100nm to 60nm. The desired radius of the spiral was set to 400*nm*, with the realized scan, illustrated in Figure 9, being elliptical and having an average radius of about 275*nm*. With these conditions, were able to scan stably at 9.7*Hz*, a nearly 2.5x improvement over the result shown in Figure 13. A few of the resulting frames are shown in Figure 15, showing the improved temporal resolution with which we are now able to observe the dissolution process. We note that at this frame rate, we now observe entire frames where the exposed regions of resist swell before their removal. We believe this combination of scan pattern, index matching, and cantilever choice generates data of a sufficient quality to begin using our technique to study the effect of process parameters and resist formulation on the resulting dissolution dynamics of the material.

4. CONCLUSION

We have developed a technique that is capable of measuring the dissolution dynamics of photoresist material with sub-10nm spatial resolution at 10Hz. This technique enables a detailed study of the resist dissolution properties, which we can use to focus on the impact of dissolution on the formation of stochastic defects such as LER, and even more catastrophic effects such as line bridges and breaks or missing contact holes. Already, we have uncovered that resist swelling is indeed present during the dissolution of a commercial EUV CAR, and that the dissolution process appears to act as a filter on LER following bulk removal of highly exposed material. Moving forward, we plan to study the impact of resist formulation as well as process parameters such as dose and developer strength or composition on the resist dissolution process. Ultimately, we aim to better understand the interplay between all these parameters and the resulting quality of the printed features. To that end, our technique has just scratched the surface.

5. ACKNOWLEDGMENTS

This work was performed at Lawrence Berkeley National Laboratory with support from Intel and Samsung through the U.S. Department of Energy under Contract No. DE-AC02-05CH11231.

Work at the Molecular Foundry was supported by the Office of Science, Office of Basic Energy Sciences, of the U.S. Department of Energy under Contract No. DE-AC02-05CH11231.

This work was supported by the Intel-sponsored CINEMA program and its mission to explore novel resist materials that will enable scaling at future lithographic nodes.

REFERENCES

[1] Hinsberg, W. D. and Meyers, S., "A numeric model for the imaging mechanism of metal oxide EUV resists," *Advances in Patterning Materials and Processes XXXIV 10146*(March 2017), 1014604 (2017).

[2] Xu, H., Blackwell, J. M., Younkin, T. R., and Min, K., "Underlayer designs to enhance the performance of EUV resists," *Advances in Resist Materials and Processing Technology XXVI 7273*(April 2009), 72731J (2009).

[3] De Silva, A., Dutta, A., Meli, L., Yao, Y., Mignot, Y., Guo, J., and Felix, N. M., "Inorganic hardmask development for extreme ultraviolet patterning," *Journal of Micro/Nanolithography, MEMS, and MOEMS 18*(01), 1 (2018).

[4] Alvi, M., Gottscho, R., Haider, A., Heo, S., Hsieh, P., Huang, C.-C., Jurczak, G., Kam, B., Kim, J. Y., Li, B., Li, D., Nguyen, H., Pan, Y., Peter, D., Shamma, N., Silva, A. D., Tan, S., Wang, E., Weidman, T., Wise, R., Wu, M., Verveniotis, E., Volosskiy, B., Yu, J., and Zaid, H., "Achieving zero EUV patterning defect with dry photoresist system," in *Advances in Patterning Materials and Processes XXXIX*, Sanders, D. P. and Guerrero, D., eds., PC12055, PC120550B, **International Society for Optics and Photonics, SPIE** (2022).

[5] Hinsberg, W. D. and Kanazawa, K. K., "Quartz crystal microbalance thin-film dissolution rate monitor," Review of Scientific Instruments 60(3), 489–492 (1989).

[6] Sekiguchi, A., Konishi, H., and Isono, M., "Observation of swelling behavior of ArF resist during development by using QCM method (2)," *Journal of Photopolymer Science and Technology 25*(4), 467–472 (2012).

[7] Itani, T. and Santillan, J. J., "In situ characterization of photoresist dissolution," *Applied Physics Express 3*(6), 3–6 (2010).

[8] Landie, G., Xu, Y., Burns, S., Yoshimoto, K., Burkhardt, M., Zhuang, L., Petrillo, K., Meiring, J., Goldfarb, D., Glodde, M., Scaduto, A., Colburn, M., Desisto, J., Bae, Y., Reilly, M., Andes, C., and Vohra, V., "Fundamental investigation of negative tone development (NTD) for the 22nm node (and beyond)," *Advances in Resist Materials and Processing Technology XXVIII 7972*(April 2011), 797206 (2011).

[9] Harumoto, M., Santillan, J. J., Itani, T., and Kozawa, T., "Dependence of photoresist dissolution dynamics in alkaline developers on alkyl chain length of tetraalkylammonium hydroxide," *Japanese Journal of Applied Physics 61*(5) (2022).

[10] Ziegler, D., Meyer, T. R., Amrein, A., Bertozzi, A. L., and Ashby, P. D., "Ideal Scan Path for High-Speed Atomic Force Microscopy," *IEEE/ASME Transactions on Mechatronics 22*(1), 381–391 (2017).

[11] "SuMMIT LER Analysis, www.lithometrix.com."

Industry Briefs

More Chip Production Needed in Europe, Infineon CEO Says

https://www.reuters.com/technology/more-chip-production-needed-europe-infineon-ceo-says-2022-11-15/

Photronics: Underappreciated Tailwinds Creating An Opportunity

https://seekingalpha.com/article/4559265-photronics-underappreciated-tailwinds-creating-an-opportunity

Global Soda Photomask Market Size 2022 Production by Recent Developments, Corporation Information, Key Raw Materials Analysis and Forecast to 2028

https://www.marketwatch.com/press-release/global-soda-photomask-market-size-2022-production-by-recent-developments-corporation-information-key-raw-materials-analysis-and-forecast-to-2028-2022-11-15

[News Zoom In] Photomask Shortage... Direct Hit on 'Automobile Chips'

https://english.etnews.com/20221108200003

High-NA EUV Complicates EUV Photomask Future

https://semiengineering.com/high-na-euv-complicates-euv-photomask-future/

The Cost of a 3nm Chip is Nearly $600 million. Where is it?

https://min.news/en/tech/def29226dea2b06f47efea4aae13e8f3.html

New Report Highlights Challenges and Opportunities Facing U.S. Semiconductor Industry

https://www.semiconductors.org/new-report-highlights-challenges-and-opportunities-facing-u-s-semiconductor-industry/

Monthly Semiconductor Sales Decrease 0.5% Globally in September

https://www.semiconductors.org/monthly-semiconductor-sales-decrease-0-5-globally-in-september/

New Report Identifies Target Areas for CHIPS R&D Investments

https://www.semiconductors.org/new-report-identifies-target-areas-for-chips-rd-investments/

TSMC Planning Advanced Chip Production in Arizona, Says Company's Founder

https://www.reuters.com/technology/tsmc-planning-advanced-chip-production-arizona-company-founder-says-2022-11-21/

Applied Materials Forecasts Strong Q1 Revenue on Easing Supply Chain Woes

https://www.reuters.com/business/applied-materials-forecasts-current-quarter-revenue-above-estimates-2022-11-17/

UK Orders Sale of Microchip Factory by China's Nexperia, Citing National Security

https://www.reuters.com/technology/uk-orders-chinas-nexperia-sell-least-86-microchip-factory-2022-11-16/

N • E • W • S

Join the premier professional organization for mask makers and mask users!

About the BACUS Group

Founded in 1980 by a group of chrome blank users wanting a single voice to interact with suppliers, BACUS has grown to become the largest and most widely known forum for the exchange of technical information of interest to photomask and reticle makers. BACUS joined SPIE in January of 1991 to expand the exchange of information with mask makers around the world.

The group sponsors an informative monthly meeting and newsletter, BACUS News. The BACUS annual Photomask Technology Symposium covers photomask technology, photomask processes, lithography, materials and resists, phase shift masks, inspection and repair, metrology, and quality and manufacturing management.

Individual Membership Benefits include:

- Subscription to BACUS News (monthly)
- Eligibility to hold office on BACUS Steering Committee

spie.org/bacushome

Corporate Membership Benefits include:

- 3-10 Voting Members in the SPIE General Membership, depending on tier level
- Subscription to BACUS News (monthly)
- One online SPIE Journal Subscription
- Listed as a Corporate Member in the BACUS Monthly Newsletter

spie.org/bacushome

CALENDAR

2023

SPIE Advanced Lithography + Patterning
26 February–2 March 2023
San Jose, California, USA
www.spie.org/al

SPIE Photomask Technology and EUV Lithography
1-5 October 2023
Monterey, California, USA
www.spie.org/puv

European Mask and Lithography Conference (EMLC)
19-21 June 2023
Dresden, Germany
www.emlc-conference.com

Photomask Japan (PMJ)
25-27 April 2023
Online only
www.photomask-japan.org

You are invited to submit events of interest for this calendar. Please send to lindad@spie.org.

SPIE, the international society for optics and photonics, brings engineers, scientists, students, and business professionals together to advance light-based science and technology. The Society, founded in 1955, connects and engages with our global constituency through industry-leading conferences and exhibitions; publications of conference proceedings, books, and journals in the SPIE Digital Library; and career-building opportunities. Over the past five years, SPIE has contributed more than $22 million to the international optics community through our advocacy and support, including scholarships, educational resources, travel grants, endowed gifts, and public-policy development. www.spie.org.

SPIE.
International Headquarters
P.O. Box 10, Bellingham, WA 98227-0010 USA
Tel: +1 360 676 3290
Fax: +1 360 647 1445
help@spie.org • spie.org

Shipping Address
1000 20th St., Bellingham, WA 98225-6705 USA

SPIE.EUROPE
2 Alexandra Gate, Ffordd Pengam, Cardiff,
CF24 2SA, UK
Tel: +44 29 2089 4747
Fax: +44 29 2089 4750
info@spieeurope.org • spieeurope.org